

STUDY ON FUEL ECONOMY AND GENERATING ENERGY OF 48V MHEV WITH TWO MOTORS

Seongmin Ha ^(a), Hyeongcheol Lee ^{*(b)}

^(a)Department of Electric Engineering, Hanyang University, 222, Wangsimni-ro, Seongdong-gu, Seoul 133-791, Korea

^(b) Division of Electrical and Biomedical Engineering, Hanyang University, 222, Wangsimni-ro, Seongdong-gu, Seoul 133-791, Korea

^(a) haha4100@hanyang.ac.kr, ^(b) hclee@hanyang.ac.kr

ABSTRACT

In this paper, 48V MHEV vehicle with P0 + P4 structure is studied. In the previous paper, the best fuel economy was obtained when the energy obtained by regenerative braking was used only for EV driving. In an actual driving environment, a power generating function by an engine is essential. Therefore, not only regenerative braking energy but also additional energy from power generation is used for EV travel. Finally, the fuel economy is evaluated according to the amount of generating energy and control tendency of generating.

Keywords: Mild hybrid electric vehicle(MHEV), Fuel economy, Generating energy

1. INTRODUCTION

In the previous paper, various fuel economy comparisons of 48V MHEV of P0+P4 structure were studied. The best fuel economy was achieved when all the electrical energy from regenerative braking was used to EV driving from the same motor specifications. (S, HA. 2017). Also, when the ratio of two motor power is different, the BSG only has power to start the engine and the higher the power of the Rear-Axle motor, the better fuel economy. Because the EV operating area is wider and regenerative braking energy is high. (S, HA. 2018).

In the actual driving environment, control is not easy to use regenerative braking energy only for EV driving. In fact, the vehicle is not driven in a defined scenario (ex: FTP 75 cycle). And there is additional electricity consumption, such as the use of air conditioners. Therefore, power generating functions using engines and BSG are essential. In this paper, several control methods of generating are divided to define simulation cases. The effect of generating on fuel economy is analyzed by comparing generating energy quantity and efficiency for each simulation case.

2. 48V MHEV SYSTEM MODELING

In this paper, 48V MHEV with P0 + P4 structure is modeled as shown in Figure 1. The models of the engine, LDC and 48 V battery applied the same

specifications as in the previous paper. And the Rear-Axle motor was 15kW and the BSG was 5kW(S, HA. 2018).

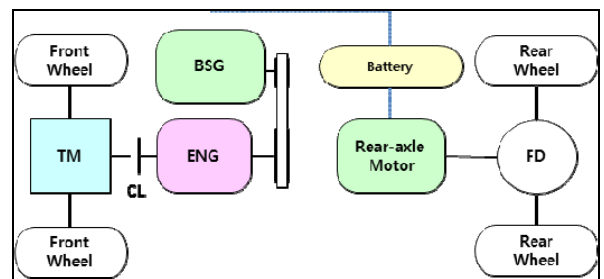


Figure 1: Target Vehicle

2.1. Engine model

Table 1 shows the specification of the engine of the target vehicle.

Table 1: Engine specification

Engine parameter	
Type	Inline 4-cylinder
Fuel type	Gasoline
Maximum torque (Nm)	168.7
Maximum power (kW)	99.54

Figure 2 represents maximum torque and BSFC(Brake Specific Fuel Consumption) at engine torque and speed conditions. As shown in Equation (1), the engine model outputs the engine output torque determined by the host controller (HCU) to the torque value between the maximum torque in the throttle maximum open state and the engine friction torque in the closed state.

$$T_{eng} = \min(T_{wott}(w_{eng}), \max(T_{HCU,eng} + T_{eng,idle}, T_{ctt}(w_{eng}))) \quad (1)$$

Where,

$$T_{eng,idle} = \max(k_p(w_{idle} - w_{eng}), 0)$$

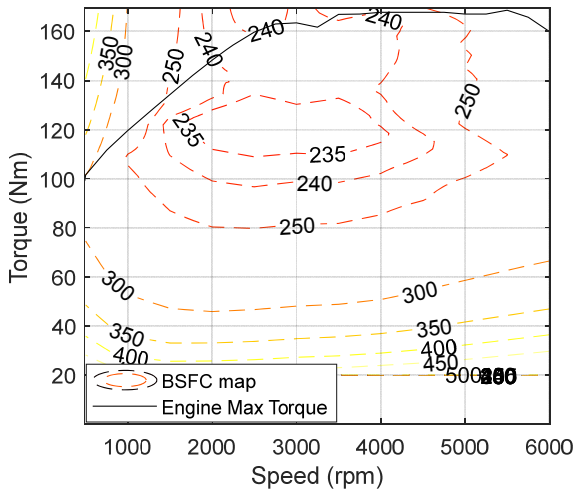


Figure 2: Engine maximum torque and BSFC map

2.2. Motor model

The motors are classified into two types according to their mounting positions. The BSG is connected to the engine by a belt. The rear-axle motor is connected to the rear reduction gear. The specifications of the two motors are as shown in Table 2.

Table 2: Electric motor specification

Electric motor parameter		
Type	BSG	Rear-axle motor
Max power (kW)	5	15
Max torque (Nm)	31.8	47.7
Base Speed (RPM)	1500	3000
Max Speed (RPM)	16000	12000

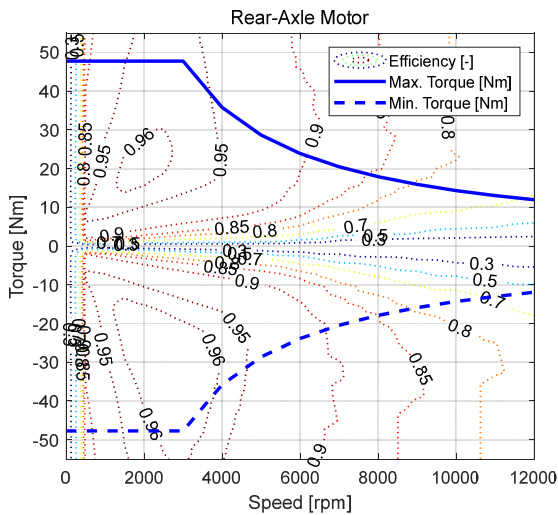


Figure 3: Max/min torque and Efficiency map of Rear-Axle motor

The drive motors mounted on the front and rear wheels have the same model structure, and the corresponding motor model reflects the motor torque command value

determined by the HCU in the output. The output torque of the motor model is limited to the maximum drive or braking torque possible at the current motor speed. The torque of the motor is expressed by Equation (2), and the power of the motor has a relationship as shown in Equation (3).

$$T_{mot} = \min(T_{\max}(w_{mot}), \max(T_{HCU, mot} - T_{\max}(w_{mot}))) \quad (2)$$

$$P_{mot} = T_{mot} \times w_{mot} \times h^k(T_{mot}, w_{mot}) \quad (3)$$

Where,

$$k = \begin{cases} 1 & (T_{mot} \times w_{mot} < 0) \\ -1 & (T_{mot} \times w_{mot} > 0) \end{cases}$$

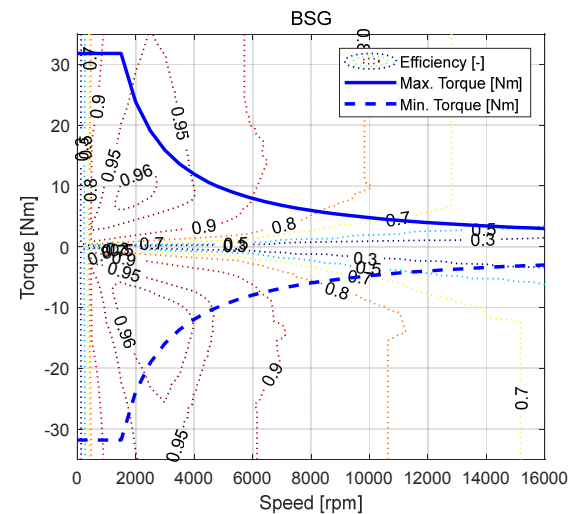


Figure 4: Max/min torque and Efficiency map of BSG

2.3. LDC model

LDC (Low Voltage DC-DC Converter) supplies power to a 12V electric field load. The 12V total field load power is 217W and the LDC efficiency is 0.95, both of which are fixed values. The LDC output power is given by Equation (4).

$$P_{LDC} = \frac{P_{Load}}{h_{LDC}} \quad (4)$$

2.4. Battery model

The 48V battery cell voltage is calculated from the open circuit voltage of the battery cell, the cell internal resistance, and the current. The temperature is assumed to be maintained at 40 °C, and the internal resistance is determined according to the direction of the current and the SOC as shown in equation (5).

$$V_{bat, cell} = V_{OCV}(SOC) - R_{int}(SOC, \text{sgn}(I_{bat})) \times I_{bat} \quad (5)$$

Where,

$$R_{int} = \begin{cases} R_{discharge} & (\text{sgn}(I_{bat}) > 0) \\ R_{charge} & (\text{sgn}(I_{bat}) < 0) \end{cases}$$

The current of the 48V battery is calculated by the equation (6) with the sum of BSG power, rear-axle motor power and LDC power divided by the battery voltage.

$$I_{bat} = \frac{P_{mot.bsg} + P_{mot.rear} + P_{LDC}}{N_{cell} \mathcal{V}_{bat.cell}} \quad (6)$$

Nominal voltage is 3.7V, and capacity is 23Ah. 13 battery cells are connected in series.

3. SUPERVISORY CONTROL ALGORITHM

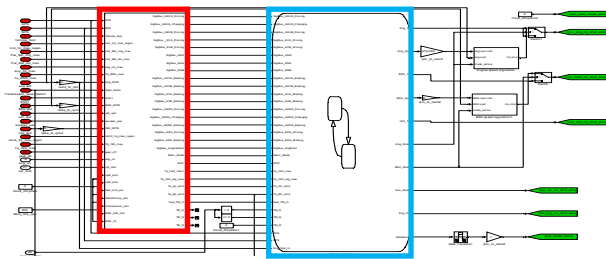


Figure 5: Supervisory control algorithm(Power distribution(red)/Mode decision(blue) algorithm)

As shown in the figure 5, the upper control algorithm was developed using Simulink, and consists of the mode decision algorithm and the power distribution algorithm of each mode. Details of driving mode and power distribution can be found in previous paper(S, Ha. 2017).

4. SIMULATION

4.1. Simulation case

The simulation case is defined as nine, as shown in Table 3. The method of control is divided into Constant torque and OOL(Optimal Operating Line) control. And they are divided into three generating energy for each. In addition, case without control of generating is included for fuel economy comparison.

Table 3: Simulation case by Generating control method

Control method : Constant torque	Control method : OOL torque
No Gen. (A)	
-10 Nm (B)	T_{ool} (F)
-7.5 Nm (C)	$0.95 T_{ool}$ (G)
-5 Nm (D)	$0.9 T_{ool}$ (H)
-2.5 Nm (E)	$0.85 T_{ool}$ (I)

The Constant torque control method uses the BSG to generate electricity at a constant torque when the engine speed is greater than 800 rpm. The OOL control method runs the engine at the OOL torque when the engine speed is more than 800 rpm. In the OOL control method, run the engine at the OOL torque when the engine speed

is more than 800 rpm. The BSG generates electricity from the driver's demand torque minus the OOL torque.

4.2. Simulation Result

The vehicle speed in all simulation cases is not significantly different from the speed of FTP75 cycle as shown in Figure 6. In Figure 7, SOC simulation results for all cases. The Final SOC for all cases is between 55% and 56%. Therefore, the fuel economy effects of the final SOC are ignored.

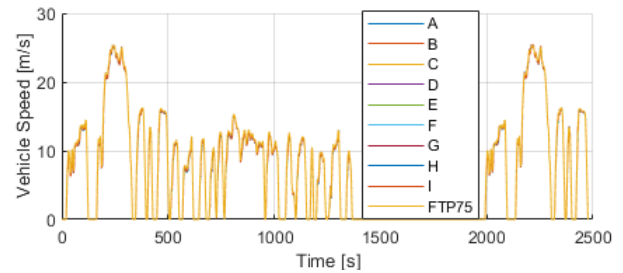


Figure 6: Simulation result - Vehicle speed

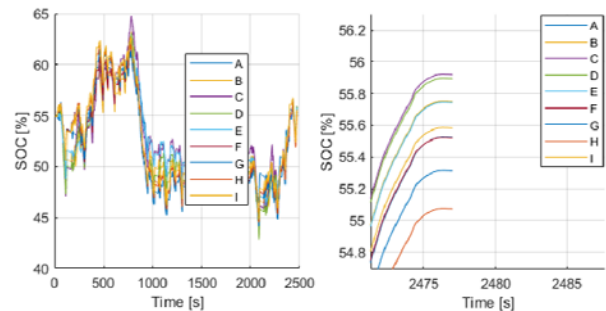


Figure 7: Simulation result - SOC of 48V battery

D

Table 4: Simulation result - Fuel economy

Simulation case	Fuel economy (km/l)	Fuel economy Improvement rate (%)
A	19.15	0
B	20.84	8.86
C	20.62	7.66
D	20.07	4.79
E	19.43	1.48
F	21.73	13.49
G	21.67	13.17
H	21.55	12.57
I	21.27	11.08

The fuel economy results for each case are shown in Table 4. Based on the results of Case A, the fuel economy improvement rate of Case B to I was calculated. Figure 8 is the engine operating point of Case A and is the basis for comparison with other cases. Figure 9 is for constant torque control (B to E) and Figure 10 is for OOL torque control (F to I).

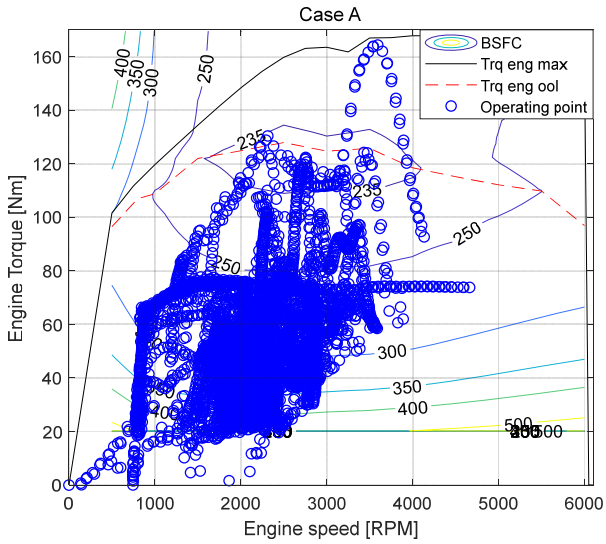


Figure 8: Engine operating point (Case A)

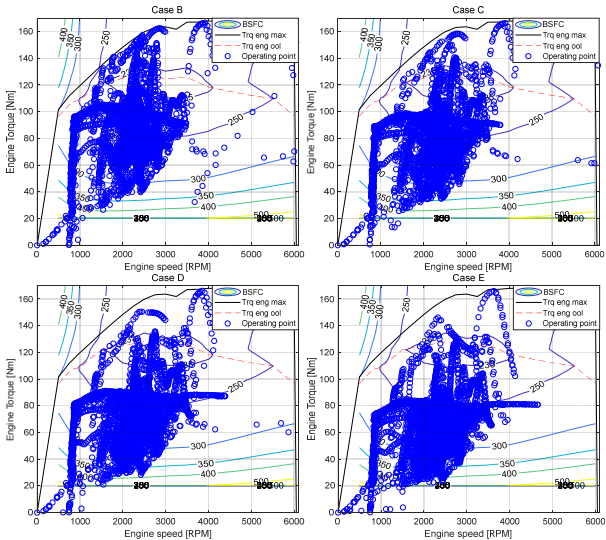


Figure 9: Engine operating point (Case B~E)

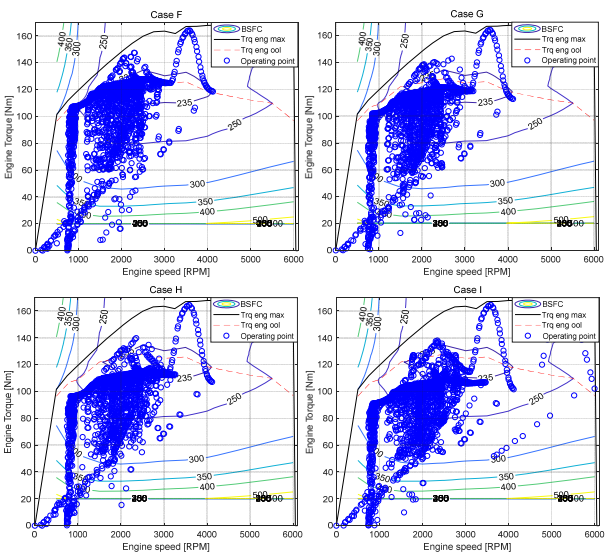


Figure 10: Engine operating point (Case F~I)

4.3. Analysis of simulation result

In Table 5, the power generation energy for each simulation case was compiled and calculated as shown in Equation (7) below.

$$E_{gen} = \int_0^T V_{BSG}(t) |I_{BSG}(t)| k_{gen} dt \quad (7)$$

Where,

$$k_{gen} = \begin{cases} 1 & (\text{Generating On}) \\ 0 & (\text{Generating Off}) \end{cases}$$

Table 5: Generating energy

Simulation case	Generating energy (kJ)
A	0
B	1798
C	1746
D	1338
E	647
F	1661
G	1651
H	1636
I	1577

More power generation energy can be obtained from cases where power control has been carried out with high torque. However, the increase in torque and the power generation energy are not directly proportional. During EV operation, power generation is not possible by turning off the engine and using the BSG. Therefore, if the power generation torque is increased, the 48V battery can be charged faster and the EV mode can be driven more. So the time for BSG to generate electricity is reduced.

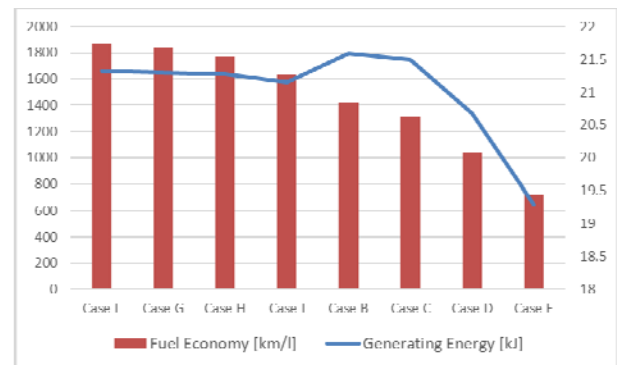


Figure 11: Fuel economy and Generating Energy

Looking at Figure 11, the case of OOL torque control (F~I) has a higher fuel economy result than that of Constant torque control (B~E). In particular, Case I has lower power generation energy but higher fuel economy than Case B and C. As Figure 12 shows, case C is caused by the engine running at a lower efficiency point than I. Figure 12 shows the engine operating points of Case E with the lowest fuel economy improvement and Case A without power generation control. Engines tend

to be less efficient at low torque. The BSG's power generation operation increases the operating torque of the engine to increase the efficiency of the engine, and uses the power generation energy to drive the EV to improve fuel economy.

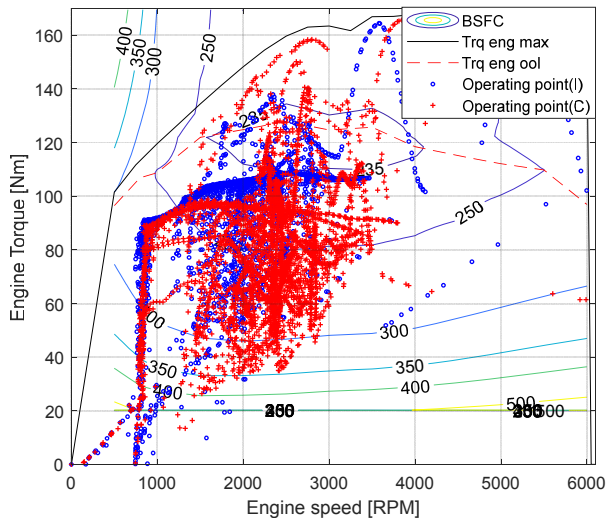


Figure 12: Operating point of Case I and C

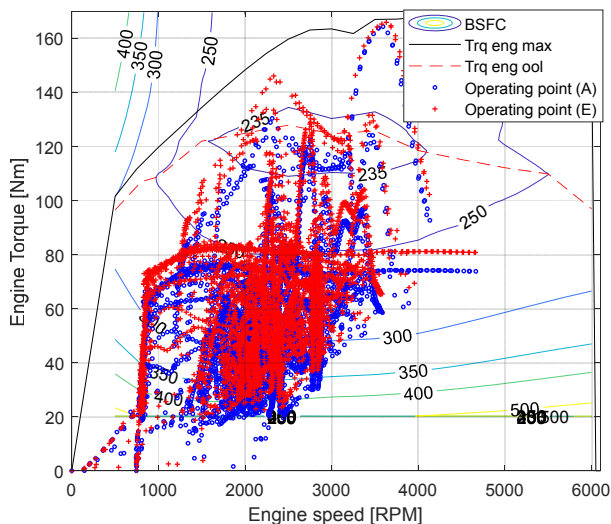


Figure 13: Operating point of Case A and E

5. CONCLUSION

In this paper, it was confirmed that the fuel economy improvement effect can be obtained when EV driven with the additional electrical energy obtained through the development of BSG in the 48V MHEV of P0+P4 structure. It is also important to obtain additional electrical energy through generating, but it is more important to run the engine at a more efficient operating point. However, since the 48V MHEV system has relatively low power, verification of the application of the OOL control in the actual vehicle, not in the simulation, is required.

ACKNOWLEDGMENTS

This work was supported by the Industrial Strategic technology development program, 20000578, A development

of optimal eco driving system in HEV/PHEV based on connected vehicle environment funded By the Ministry of Trade, industry & Energy(MI, Korea).

REFERENCES

- S, Ha., T, Park., W, Na., and H, Lee., "Power distribution control algorithm for fuel economy optimization of 48V mild hybrid vehicle," Proc. of the Int. Conference on Modeling and Applied Simulation, 2017, ISBN 978-88-97999-91-1, 185-190.
- S, Ha., W, Na., and H, Lee., "Study on economy and regenerative braking of 48V mild hybrid vehicle with two motors," Proc. of the Int. Conference on Modeling and Applied Simulation, 2018, ISBN 978-88-85741-07-2, 22-26.
- Kuypers, M., "Application of 48 Volt for Mild Hybrid Vehicles and High Power Loads," SAE Technical Paper2014-01-1790, 2014, doi:10.4271/2014-01-1790.
- Bao, R., Avila, V., and Baxter, J., "Effect of 48V Mild Hybrid System Layout on Powertrain System Efficiency and Its Potential of Fuel Economy Improvement," SAE Technical Paper 2017-01-1175, 2017.